# Fragmentation of valence electronic states of CF3-CH2F+ and CHF2-CHF2+ in the range 12-25eV

Zhou, Weidong; Seccombe, Dominic; Tuckett, Richard

*Document Version*
Peer reviewed version

Link to publication on Research at Birmingham portal

Threshold photoelectron-photoion coincidence spectroscopy of the hydrofluorocarbons
$CF_3$-$CFH_2^+$ and $CF_2H$-$CF_2H^+$ in the range 12-25 eV

W. Zhou, D.P. Seccombe and R.P. Tuckett *

Professor Richard Tuckett  (University of Birmingham)  /  July 2011

# Fragmentation of valence electronic states of $CF_3-CH_2F^+$ and $CHF_2-CHF_2^+$ in the range 12-25 eV (v2 after comments of referees)

## Weidong Zhou,[a] D.P. Seccombe [b] and R.P. Tuckett

*School of Chemical Sciences, University of Birmingham, Edgbaston, Birmingham, B15 2TT, U.K.*

[a] Present address : Department of Chemistry, University of California Riverside, CA 92521-0403, USA
[b] Present address : Department of Physics, Newcastle University, Newcastle-upon-Tyne, NE1 7RU, UK

Number of pages :     20  (excluding tables and figures)
Number of tables :     3
Number of figures :     7

Author for correspondence :  Dr R P Tuckett
         [email: r.p.tuckett@bham.ac.uk, fax: +44 121 414 4426]

-----------------------------------------------------------------------------------------------------------------

Tunable vacuum-ultraviolet radiation from a synchrotron source and threshold photoelectron-photoion coincidence spectroscopy have been used to study the decay dynamics of the valence electronic states of $CF_3-CH_2F^+$ and $CHF_2-CHF_2^+$.  The threshold photoelectron spectra, fragment ion yield curves, and breakdown diagrams of $CF_3-CH_2F$ and $CHF_2-CHF_2$ have been obtained in the photon energy range 12-25 eV, the electrons and fragment ions being detected by a threshold electron analyser and a linear time-of-flight mass spectrometer, respectively.  For the dissociation products of $(CF_3-CH_2F^+)^*$ and $(CHF_2-CHF_2^+)^*$ formed *via* a single-bond cleavage, the mean translational kinetic energy releases have been measured and compared with the predictions of statistical and pure-impulsive mechanisms.  *Ab initio* G2 calculations have determined the minimum-energy geometries of $CF_3-CH_2F$ and $CHF_2-CHF_2$ and their cations, and deduced the nature of the high-lying valence orbitals of both neutral molecules.  Furthermore, enthalpies of formation at 298 K of both neutral molecules, and all the neutral and fragment ions observed by dissociative photoionisation have been calculated.  Combining all experimental and theoretical data, the decay mechanisms of the ground and excited valence states of $CF_3-CH_2F^+$ and $CHF_2-CHF_2^+$ are discussed.  The first and second excited states of both ions show some evidence for isolated-state behaviour, with fast dissociation by cleavage of a C–F or C–H bond and a relatively large translational energy released in the two fragments.  The ground state of both ions dissociate by cleavage of the central C–C bond, with a much smaller translational energy release.  Several fragment ions are observed which form *via* H-atom migration across the C–C bond ; for hν > 18 eV, $CH_2F^+$ is even the dominant ion from dissociative photoionisation of $CHF_2-CHF_2$.  New experimental values are determined for the enthalpy of formation at 298 K of $CF_3-CH_2F$ ($-905 \pm 5$ kJ mol⁻¹), $CHF_2-CHF_2$ ($-861 \pm 5$ kJ mol⁻¹), $CF_2-CH_2F^+$ ($\le 485 \pm 7$ kJ mol⁻¹), $CF_2-CHF_2^+$ ($\le 324 \pm 7$ kJ mol⁻¹) and $CHF-CHF_2^+$ ($\le 469 \pm 7$ kJ mol⁻¹).

# 1. Introduction

Several fluorinated ethanes have been proposed as acceptable replacements for the banned chlorofluorocarbons.[1] These compounds include the hydrofluorocarbons (HFCs) 1,1 difluoroethane (R152a), 1,1,1,2 tetrafluoroethane (R134a) and pentafluoroethane (R125). 1,1,1,2 tetrafluoroethane has already been used for some time as a replacement for $CF_2Cl_2$ in automative air conditioning systems.[2] HFCs have been proposed as alternatives to CFCs because the presence of C–H bonds causes them to react faster with the OH radical in the troposphere, thereby reducing their lifetime in the earth's atmosphere. They also lack chlorine and bromine atoms which can catalyse the removal of ozone in the stratosphere. Even though HFCs do not contribute to ozone destruction, they still pose a threat to the environment because of their potential to contribute to global warming.[3] If the reaction of the HFC with the OH radical is sufficiently slow, the removal of these species from the atmosphere may be governed by photoionisation and photodissociation processes that occur in the mesosphere. A knowledge of the vacuum-UV (VUV) photochemistry of HFCs which might take place in this region of the atmosphere is therefore important.

Our group is investigating the decay dynamics of a range of halocarbon and HFC cations containing at least two carbon atoms, using threshold photoelectron photoion coincidence (TPEPICO) spectroscopy with synchrotron radiation as a tunable VUV photoionisation source. To date, we have studied a range of saturated and unsaturated perfluorocarbons, $C_xF_y^+$,[4,5], and one HFC, $CHF_2–CF_3^+$.[6] In this paper, we report data for the two isomers of the tetrafluoroethane cation ; $CF_3–CH_2F^+$ (labelled 1,1,1,2) and $CHF_2–CHF_2^+$ (labelled 1,1,2,2). Preliminary results have been reported elsewhere.[7] The limited studies of these two isomers of tetrafluoroethane have all focused on their structure, conformational stability, and spectroscopy of the neutral molecule. These investigations include microwave, electron diffraction, IR and Raman studies, as well as *ab initio* calculations.[8-16] In this paper we describe the results of a TPEPICO study of $CF_3–CH_2F$ and $CHF_2–CHF_2$ from the onset of ionisation (*ca.* 12 eV) to 25 eV. The first threshold photoelectron spectra (TPES) and state-selected fragmentation studies of the parent ions are presented. Breakdown diagrams, yielding the formation probability of fragment ions as a function of photon energy, are obtained. The mean translational kinetic energy releases for unimolecular fragmentation proceeding *via* a single-bond cleavage are determined, and compared with the predictions of statistical and dynamical impulsive models. Enthalpies of formation at 298 K for the two neutral isomers and some fragment ions are also determined. These experimental results are complemented and compared with *ab initio* calculations of the structure of the two isomers of tetrafluoroethane, their ionisation energies, and the enthalpy of formation of several fragment ions.

# 2. Theoretical and experimental methods

## 2.1 Computational methods

Using Gaussian 98, *ab initio* molecular orbital calculations have been performed for $CF_3$–$CH_2F$ and $CHF_2$–$CHF_2$, both in their neutral ground states and in the ground states of the parent cations. Calculations have also been performed for fragments produced by VUV dissociative photoionisation (*e.g.* $CF_2$–$CH_2F^+$, $CF_3$). Structures for all species were optimised using the second-order Møller-Plesset theory (MP2) with the 6-31G(d) basis set, and all electrons were included at the MP2(full)/6-31G(d) level. The MP2(full)/6-31G(d) structures were then employed for energy calculations according to the Gaussian-2 (G2) theoretical procedure.[17] This procedure involves single-point total energy calculations at the MP4/6-311G(d,p), QCISD(T)/6-311g(d,p), MP4/6-311G(d,p), MP4/6-311G(2df,p), and MP2/6-311G(3df,2p) levels. A small empirical correction is employed to include the high-level correlation effects in the calculations of the total electronic energies (EE). The HF/6-31G(d) harmonic vibrational frequencies, scaled by 0.8929, are applied for zero-point vibrational energy (ZPVE) corrections to obtain the total energies at 0 K ($E_0 = EE + ZPVE$). The enthalpies of formation at 298 K ($\Delta_f H^o_{298}$) for molecular species are calculated using the scaled HF/6-31G(d) harmonic frequencies, leading to predicted enthalpies of unimolecular reactions (*e.g.* $CF_3$–$CH_2F \rightarrow CF_2$–$CH_2F^+ + F + e^-$). The agreement between G2 and experimental results is usually well within $\pm$ 0.2 eV (or $\pm$ 20 kJ mol$^{-1}$).[17]

## 2.2 Experimental methods

The TPEPICO apparatus has been described in detail elsewhere,[18,19] and only a brief outline is given here. Synchrotron radiation from the 2 GeV electron storage ring at the Daresbury Laboratory is energy-selected using a 1 m Seya-Namioka monochromator equipped with two gratings, covering the energy range *ca.*8-40 eV. The majority of these experiments were performed using the higher-energy grating (range 105-30 nm (12-40 eV), blaze *ca.*55 nm) with an optical resolution of 0.3 nm. With this grating the effects of second-order radiation are insignificant over the chosen photon energy range. The wavelength of the monochromater was calibrated with the energies of the $^2P_{3/2}$ (15.759 eV) and $^2P_{1/2}$ (15.937 eV) states of Ar$^+$. The VUV radiation is admitted into the interaction region through a glass capillary, and the photon flux is monitored using a photomultiplier tube *via* the visible fluorescence from a sodium salicylate-coated window.

Threshold photoelectrons and fragment cations produced by photoionisation are extracted in opposite directions by a 20 V cm$^{-1}$ electric field applied across the interaction region, and detected by a single channel electron multiplier and microchannel plates, respectively. The threshold electron analyser consists of a cylindrical electrostatic lens designed with large chromatic aberrations and a 127° post-analyser to reject energetic electrons emitted on axis. The operating resolution is 10 meV,[19] degraded

from the initial design of *ca.* 3 meV [18] by increasing the size of the aperture to the post-analyser. Since the optical resolution of 0.3 nm corresponds to 35-140 meV in the photon range 12-24 eV, the resolution of the experiment is determined by that of the photon source, not that of the electron analyser. Positive ions from the interaction region are extracted and pass through a linear time-of-flight (TOF) mass spectrometer of the Wiley-Maclaren design.[20] Following discrimination and pulse shaping, signals from the electron and ion detectors pass to a time-to-digital converter (TDC) configured in the multi-hit mode and mounted in a PC. The electrons provide the 'start', the ions the 'stop' pulses, allowing signals from the same ionisation process to be detected in delayed coincidence.

TPEPICO spectra are recorded either continuously as a function of photon energy or at a fixed energy. In the scanning-energy mode, flux-normalized TPEPICO spectra are recorded as three-dimensional, false-color maps, where the coincidence count is plotted against ion flight time and photon energy. By taking cuts through the histogram in different ways, two spectra are obtained. A cut through the map at a fixed photon energy yields the time of flight mass spectrum (TOF-MS), which identifies the fragment ions formed in the dissociative photoionisation at that energy. Alternatively, a background-subtracted cut taken through the histogram at a fixed flight time, corresponding to a mass peak in the TOF-MS, gives an ion yield curve. The breakdown diagram, showing the formation probability of the product ions as a function of photon energy, can then be calculated through normalization of the ion intensities at every energy. In this mode of operation, the TOF resolution is degraded so that *all* the fragment ions are observed simultaneously. The variation of sensitivity with ion mass of this apparatus over the range 31 u ($CF^+$, the lightest ion observed) to 102 u (parent ion) does not significantly affect the breakdown diagram.[4] The threshold electron and total ion counts are also recorded, yielding the TPES and total ion yield curve, respectively.

In the fixed-energy mode, TOF spectra (later referred to as TPEPICO-TOF spectra) are measured at *single* energies corresponding to peaks in the TPES. By contrast with the scanning-energy mode, a TOF resolution as high as the signal level permits is employed, and usually only one fragment ion is observed per spectrum. Fragment ions often have enough translational energy for the peaks comprising the TPEPICO-TOF spectra to be substantially broadened. From an analysis of the peak shape, it is then possible to obtain kinetic energy release distributions (KERDs) and hence mean kinetic energy releases, $<KE>_T$.[21,22]

The sample gases, $CF_3-CH_2F$ and $CHF_2-CHF_2$, were obtained commercially (Fluorochem Ltd., UK), with a stated purity of >99% and used without further purification. The operating pressure varied from 2 to $5 \times 10^{-5}$ Torr.

## 3. Theoretical results

### 3.1 Structure of $CF_3-CH_2F$ and $CF_3-CH_2F^+$

The optimised geometry of $CF_3-CH_2F$ has been determined at the MP2/6-31(d) level. The molecule adopts a staggered structure of $C_s$ symmetry with four atoms (F1, C1, C2, F4) lying in the symmetry plane. Second-derivative calculations were performed at the optimised geometry to ensure it corresponded to a genuine energy minimum ; this geometry was confirmed by determining 18 real harmonic vibrational frequencies. The structural parameters, listed in Table 1, are in good agreement with microwave, [8] electron diffraction, [10] and other *ab initio* studies.[12,14] Similarly, the ground state of $CF_3-CH_2F^+$ is calculated to adopt a staggered structure with $C_s$ symmetry (Table 1). At this level of theory, the main changes in geometry between the ground state of $CF_3-CH_2F$ and its cation are an increase in C−C bond length by 0.43 Å, a decrease in the C−F bond length by 0.06 and 0.08 Å in the $CF_3-$ and $-CH_2F$ groups respectively, and almost no change in C−H bond length. In addition, both the $CF_3-$ and $-CH_2F$ groups adopt a more planar structure upon ionisation.

The electronic configuration of $CF_3-CH_2F$ $\tilde{X}$ $^1A'$ is ….. $(6a'')^2(16a')^2(7a'')^2(8a'')^2(17a')^2$, where the numbering includes core orbitals. The structure of the neutral molecule and its three highest valence molecular orbitals (MOs) are shown in Figure 1. The 17a' highest-occupied molecular orbital (HOMO) forms predominantly from s orbitals on carbon and hydrogen atoms, and p orbitals on fluorine. It has strong C−C σ-bonding with some C−F and C−H σ*-antibonding character. In addition, there is some π* antibonding contribution localised on the $-CH_2F$ group with a node perpendicular to the symmetry plane. Upon electron removal to form $CF_3-CH_2F^+$ $\tilde{X}$ $^2A'$, a significant increase in the C−C and a small decrease in the C−F bond lengths are predicted. From the Franck-Condon principle, therefore, vibrational excitation of the cation is expected upon ionisation, particularly in the C−C stretching mode but also in the $CF_3$ and $CH_2F$ umbrella modes. From the G2 values for the total energies at 0 K ($E_o$) of $CF_3-CH_2F$ and its cation, both calculated at their respective minimum-energy geometries, the adiabatic ionisation energy (AIE) of $CF_3-CH_2F$ is determined to be 12.25 eV. The unfavourable Franck-Condon factors at the onset of the first photoelectron band will almost certainly lead to an experimental onset of signal which is significantly greater than this *ab initio* value.[23] Assuming the same geometry for $CF_3-CH_2F^+$ $\tilde{X}$ $^2A'$ as for the neutral molecule, the vertical ionisation energy (VIE) is calculated to be 13.96 eV.

The orbital of next highest energy (*i.e.* HOMO-1), 8a'', forms predominantly from C−H σ-bonding and F 2pπ lone-pair orbitals. It also exhibits π* antibonding character on the $-CH_2F$ group, with a node in the symmetry plane. The (HOMO-2) orbital, 7a'', forms solely from F 2pπ lone-pair orbitals. This orbital is

6

largely localised on the $CF_3-$ group. The removal of an electron from this localised orbital is expected to result in C−F bond fission, *i.e.* fragmention to $CF_2-CH_2F^+ + F$, provided the dissociation follows a rapid impulsive mechanism.

## 3.2   Structure of $CHF_2-CHF_2$ and $CHF_2-CHF_2^+$

The structural parameters and the optimised geometry of $CHF_2-CHF_2$ are shown in Table 1 and Figure 2, respectively. The parameters for the cation are also shown in Table 1. Second-derivative calculations confirm that the optimised geometries do correspond to true energy minima. The calculations predict that both $CHF_2-CHF_2$ and its cation have trans structures of $C_{2h}$ symmetry, with the two hydrogen and two carbon atoms lying in the symmetry plane (Fig. 2). The structural parameters for the neutral molecule are very close to the results of electron diffraction [9] and other *ab initio* studies.[14,15] There is no reported microwave spectrum of this isomer. As with the 1,1,1,2 isomer, ionisation is accompanied by a large increase in C−C bond length (+0.44 Å), a smaller decrease in C−F length (−0.07 Å), and almost no change in C−H length. In addition, the geometry of the two $CHF_2-$ groups becomes closer to planar.

The electronic configuration of $CHF_2-CHF_2$ $\widetilde{X}$ $^1A_g$ is  ….. $(5a_u)^2(5b_g)^2(7a_g)^2(7b_u)^2(8a_g)^2$. As with the 1,1,1,2 isomer, it is difficult to give a simple characterisation of the MOs due to the mixing of bonding interactions with lone pairs. As in the 1,1,1,2 isomer, the HOMO can be characterised as C−C σ bonding with some C−H and C−F antibonding contributions. Electron loss from this orbital leads to formation of the ground state of $CHF_2-CHF_2^+$, and all the comments made in the preceding section about the vibrational excitation in the first photoelectron band apply equally here. Using the same procedure as described above, the AIE of $CHF_2-CHF_2$ is calculated to be 11.77 eV, *ca.* 0.5 eV lower than that of $CF_3-CH_2F$. The VIE of the 1,1,2,2 isomer is calculated to be 13.12 eV.

The (HOMO-1) orbital, $7b_u$, has most contribution from p orbitals on the fluorine and carbon, and s orbitals on hydrogen atoms. It shows some C−H bonding and F $2p\pi$ non-bonding character. We note that electron removal from this orbital, followed by rapid impulsive dissociation, might be expected to break either the C−H or the C−F bonds, forming $CF_2-CHF_2^+ + H$ or $CHF-CHF_2^+ + F$, respectively (Section 4.2.2). The (HOMO-2) orbital, $7a_g$, has strong C−H and C−C bonding character, with some F $2p\pi$ bonding to the carbon atoms.

## 3.3   Calculation of $\Delta_r H^o_{298}$ for dissociative photoionisation reactions

As described in Section 2.1, the enthalpies of formation at 298 K of both isomers of $C_2F_4H_2$, and all the neutral and fragment ions observed by dissociative photoionisation have been calculated. It is therefore possible to calculate the enthalpy of reaction at this temperature for all of the observed dissociative

photoionisation reactions. For reactions involving a single bond fission, which we describe as production of the *major* fragment ions, these values are shown in Table 2 Column 4. Note that these calculations relate to geometries of both reactants and products that are optimised by the G2 procedure.

## 4. Experimental results

### 4.1 Threshold photoelectron spectra of CF$_3$–CH$_2$F and CHF$_2$–CHF$_2$

The TPES of the two isomers of C$_2$F$_4$H$_2$ in the range 12-25 eV at an optical resolution of 0.3 nm are shown in Figures 3(a) and 4(a). The coincidence ion yield curves, shown in figures 3(b-c) and 4(b-c) , are discussed later. In both spectra, as with CHF$_2$–CF$_3$,[6] the lowest-energy peak (*ca.* 12-15 eV) corresponding to the ground electronic state of the parent ion is relatively weak. In the energy range 15-18 and 19-22 eV two intense series of bands are observed. Molecular orbital calculations suggest that these result from the overlap of several excited ionic states. Finally, a weak peak at *ca.* 23 eV is common to both spectra. The similar peak positions and intensity distribution of the two spectra suggest that electrons are being removed from orbitals that have similar character and relative ordering in the two molecules.

The HOMOs of both molecules are predominantly of C–C σ bonding character, as is also true for CHF$_2$–CF$_3$ [6] and CF$_3$–CF$_3$.[4,24,25] The large width of this band in both spectra is consistent with the predicted increase in C–C bond length upon ionisation. We note, however, that this band is both weaker and broader in CHF$_2$–CHF$_2$ than in CF$_3$–CH$_2$F, which may reflect subtle differences in the nature of the HOMOs on account of the different symmetries of the two molecules. The observed onsets of ionisation for CF$_3$–CH$_2$F and CHF$_2$–CHF$_2$ are 12.64 ± 0.05 and 12.18 ± 0.05 eV, respectively. The G2 calculations also predict a higher ionisation energy for the 1,1,1,2 isomer, and a difference in AIE (0.48 eV) which is almost identical to that observed experimentally (0.46 eV). However, both experimental values are *ca.* 0.4 eV higher than the calculated values. This highlights the well-known difficulty in observing the true ionisation energy of a molecule when there is a significant change in geometry upon ionisation, and hence a vanishingly small Franck-Condon factor at threshold.[23] Under these circumstances, the observed onset of ionisation can only give a relatively crude upper limit to the true AIE. The experimental vertical ionisation energies, corresponding to the peaks of the first photoelectron bands, of 14.01 ± 0.05 (for 1,1,1,2) and 13.00 ± 0.05 (for 1,1,2,2) eV are in good agreement with the computed G2 values of 13.96 and 13.12 eV, respectively. This inspires confidence in the calculations.

The TPES of CF$_3$–CH$_2$F shows a particularly narrow peak at 17.1 eV. Narrow peaks in photoelectron spectra where vibrational structure is not resolved usually relate to the removal of a non-bonding electron,

confirming the fact that the third-highest molecular orbital of this molecule, 7a'', is essentially comprised of a F 2p$\pi$ lone-pair orbital.


## 4.2 Scanning-energy TPEPICO spectra

TPEPICO spectra in the scanning-energy mode were recorded for $CF_3-CH_2F$ and $CHF_2-CHF_2$ from *ca.* 12-25 eV at an optical resolution of 0.3 nm and a TOF resolution of 64 ns. The ion yield curves are shown in Figures 3(b)-3(c) and 4(b)-4(c), respectively. The corresponding breakdown diagrams are shown in Figures 5 and 6. In this paper we classify the ion products into two groups ; the *major* ions which constitute the parent ion and the fragment ions produced by the cleavage of a single bond, and the *minor* ions which constitute the fragment ions produced by the cleavage of more than one bond and the possible simultaneous formation of bond(s). The 298 K appearance energies ($AE_{298}$) for the major and minor ions from both isomers of $C_2F_4H_2$ have been determined from the extrapolation of the linear portion of the ion yield to zero signal. They are shown in Table 2 Column 2. At the resolution of our experiment, this is equivalent to the first onset of signal. No corrections have been made for exit-channel barriers or kinetic shifts, and AEs determined in this way can only be regarded as upper limits. We have used the procedure of Traeger and McLoughlin [26] to convert the $AE_{298}$ of the major fragment ions into an enthalpy of the unimolecular reaction at 298 K, $\Delta_r H^o_{298}$, shown in Table 2 Column 3. Full details are given elsewhere.[6,26,27] Experimental values for $\Delta_f H^0_{298}$, given in brackets in Column 1 of Table 2, were taken from Chase [28] or Lias *et al.*[29], the exceptions being the values used for $CF_3$,[30] $CF_3^+$,[31] and $CHF_2^+$.[6] For fragments with one carbon atom, there is excellent agreement between these values of $\Delta_f H^o_{298}$ and those calculated by the G2 procedure, always less than 20 kJ mol$^{-1}$. The values of $\Delta_f H^0_{298}$ used for the parent neutral molecule, $-905$ kJ mol$^{-1}$ for $CF_3-CH_2F$ and $-861$ kJ mol$^{-1}$ for $CHF_2-CHF_2$, were deduced from the $AE_{298}$ data for the major fragment ions (see below). They are in good agreement with earlier literature values of $-896$ [16] and $-875$ [15] kJ mol$^{-1}$, respectively. The agreement with our G2 values, -932 and $-905$ kJ mol$^{-1}$, is less satisfactory.


### 4.2.1 Coincidence ion yields of $CF_3-CH_2F^+$ Unlike $CF_3-CF_3^{+\ [4,24,25]}$ and $CHF_2-CF_3^{+,[6]}$ the parent ion is observed in the low-energy part of the Franck-Condon region of the ground state of $CF_3-CH_2F^+$. Over the range 12.64-12.99 eV, the parent ion forms with a relative yield of unity. A fixed-energy TPEPICO-TOF spectrum measured at 12.95 eV with improved TOF resolution shows a Gaussian-shaped peak whose width, fwhm=192 ns, is exactly that expected for a parent ion of mass 102 u extracted by a field of 20 V cm$^{-1}$ at a temperature of 298 K.[32,33] The lower region of the ground state of the ion is therefore bound, and all dissociation channels have energies greater than 12.99 eV. At a slightly higher energy within the Franck-Condon region, the major ions $CH_2F^+$ and $CF_3^+$ are observed with similar $AE_{298}$ values of $12.99 \pm 0.05$ and $13.12 \pm 0.05$ eV (Fig. 3(c)). At the Franck-Condon maximum of 14.01 eV, these two

major ions have a relative yield of *ca.* 0.5 each. They form by cleavage of the C−C bond, and are the expected products for dissociation following electron removal from the C−C σ-bonded HOMO of $CF_3$−$CH_2F$. Using the procedure of Traeger and McLoughlin [26] and assuming two reaction products only, these two $AE_{298}$ values can be converted into upper limits for the enthalpy of the corresponding unimolecular reactions of $13.15 \pm 0.05$ and $13.29 \pm 0.05$ eV, from which a mean value for $\Delta_f H^o_{298}(CF_3$−$CH_2F)$ of $-905 \pm 5$ kJ mol$^{-1}$ is determined. From the measured onset of ionisation, 12.64 eV, we can also determine $\Delta_f H^o_{298}(CF_3$−$CH_2F^+) \leq 315$ kJ mol$^{-1}$. The G2 calculation yields 251 kJ mol$^{-1}$ for the enthalpy of formation of this parent ion at 298 K.

Over the Franck-Condon regions of the first and second excited states of $CF_3$−$CH_2F^+$, the relative yield of both $CH_2F^+$ and $CF_3^+$ drops, and that of $CF_2$−$CH_2F^+$ or $CF_3$−$CH_2^+$ increases (Fig. 3(c)). At 16.0 eV the ion of mass 83 u is dominant with a relative yield of *ca.* 0.7 (Fig. 5). It is not possible to differentiate the two isomers $CF_2$−$CH_2F^+$ and $CF_3$−$CH_2^+$ in the TOF-MS. The *ab initio* calculations suggest that the former is likely to be dominant from dissociation of the $\widetilde{B}$ state, the latter might be dominant from the $\widetilde{A}$ state. Energetically, there is little difference in the calculated G2 energies of the two dissociation channels $CF_2$−$CH_2F^+ + F + e^-$ (13.90 eV) and $CF_3$−$CH_2^+ + F + e^-$ (14.07 eV). Formation of the other isomer with mass 83 u, $CHF_2$−$CHF^+$, involves both fission of a C−F bond and H-atom migration, and seems unlikely. The $AE_{298}$ of the ion of mass 83 u is $15.07 \pm 0.07$ eV, corresponding to $\Delta_r H^o_{298} \leq 15.23 \pm 0.07$ eV,[26] and the onset is steep. Since this energy corresponds to the onset of the $\widetilde{A}$ state of $CF_3$−$CH_2F^+$, and the ion yield of this fragment ion follows closely the threshold photoelectron signal over the range 15.0 to 17.5 eV which encompasses two distinct peaks, it seems likely that $CF_3$−$CH_2^+$ or $CF_2$−$CH_2F^+$ is produced directly and impulsively from the $\widetilde{A}$ and $\widetilde{B}$ states of the parent ion without prior internal conversion to the ground state. This conclusion is consistent with the relatively large kinetic energy released into $CF_3$−$CH_2^+$ or $CF_2$−$CH_2F^+ + F$ (Section 4.3), and with the MO calculation predicting that at least the $\widetilde{B}$ state is produced by electron removal from a F 2pπ non-bonding orbital on the $CF_3$−group. (There may also be a competing internal conversion decay mechanism from $\widetilde{B}$ to $\widetilde{A}$, followed by dissociation from the $\widetilde{A}$-state surface.) From the upper limit for $\Delta_r H^o_{298}$ of $15.23 \pm 0.07$ eV, we determine $\Delta_f H^o_{298}(CF_2$−$CH_2F^+) \leq 485 \pm 7$ kJ mol$^{-1}$, and for simplicity henceforth we assume that this is the dominant isomer of mass 83 u. There is no literature value with which to compare this result, so we cannot determine an independent value of $\Delta_r H^o_{298}$ for the reaction $CF_3$−$CH_2F \rightarrow CF_2$−$CH_2F^+ + F + e^-$. However, since the dissociation $CF_3$−$CH_2F^+ \rightarrow CF_2$−$CH_2F^+ + F$ has a considerable kinetic energy release, it is likely that the enthalpy of formation of this ion is significantly lower than this value. The *ab initio* G2 calculation, for instance, predicts $\Delta_f H^o_{298}(CF_2$−$CH_2F^+)$ to be 330 kJ mol$^{-1}$. We should note that

the reaction $CF_3-CH_2F \rightarrow CF_3-CHF^+ + H + e^-$, calculated by the G2 method to be open for photon energies greater than 14.09 eV, is not observed.

Above 17.5 eV the relative yield of $CF_2-CH_2F^+$ drops, and $CH_2F^+$ becomes the dominant ion again. Its ion yield follows the threshold photoelectron spectrum in the range 18-21 eV, with peaks appearing in both spectra at 18.0, 20.1 and 20.7 eV. The relative yield of $CF_3^+$ is much smaller over this photon range than over the range corresponding to the ground state of $CF_3-CH_2F^+$. Above 20 eV, from asymmetry in the peak shape, there is some limited evidence for a very small contribution of $CHF^+$ to the ion yield of $CH_2F^+$. Above 21 eV the yield of $CH_2F^+$ drops rapidly. At 23.0 eV, the energy of a weak peak in the TPES, the fragment ions are $CF^+$, $CHF_2^+$ (two minor ions - see below) and $CF_3^+$ with approximately equal relative yields.

Above 16 eV weaker, *minor* ions are observed with TOFs of 9.80, 12.55 and 14.05 μs. Using the values of the TOFs of the major ions as calibrants, these ions are predicted to have masses of 31, 51 and 64 u. They are assigned to $CF^+$, $CHF_2^+$ and $CF_2-CH_2^+$, although there is some uncertainty in the number of hydrogen atoms in all three fragments due to insufficient resolution in the TOF analyser. The $AE_{298}$ of $CHF_2^+$ is 16.11 ± 0.07 eV, and its ion yield is shown in Figure 3(b). The TOF of this ion is identical to that of the major ion formed from C–C bond fission by dissociative photoionisation of $CHF_2-CHF_2$ where the $AE_{298}$ is 12.57 eV (Section 4.2.2). This confirms the identity of the ion from $CF_3-CH_2F$ to be $CHF_2^+$. Since the $AE_{298}(CHF_2^+)$ from the two isomers is so different, the signal from the 1,1,1,2 isomer cannot be due to an impurity of the 1,1,2,2 isomer. It must arise from photon-induced fragmentation of $CF_3-CH_2F$, and therefore involves H-atom migration across the C–C bond. The possible neutral fragments associated with $CHF_2^+$ are shown in Table 2. Three channels are energetically allowed, all involving the simultaneous breaking and forming of bonds. Formation of $CHF_2^+ + CHF_2 + e^-$ ($\Delta_r H^o_{298} = 13.18$ eV) seems unlikely since both fluorine and hydrogen atoms would need to migrate across the C–C bond. It is more likely that $CHF_2^+$ forms with either $CF + HF + e^-$ ($\Delta_r H^o_{298} = 15.46$ eV) or $CF_2 + H + e^-$ ($\Delta_r H^o_{298} = 16.01$ eV). Channels to $CHF + F + e^-$ and $CH + F_2 + e^-$ are energetically closed. The yield of $CF_2-CH_2^+$ (64 u) is not shown in Figure 3 because it cannot be resolved completely from that of the stronger $CF_3^+$ (69 u) signal in the false-color map, however an $AE_{298}$ of 16.57 ± 0.07 eV can be determined. The neutral partners can either be $F_2$ or 2F, and it seems likely that each tetrahedral group of $CF_3-CH_2F$ loses one fluorine atom. From Table 2 it is clear that $CF_3-CH_2F \rightarrow CF_2-CH_2^+ + F_2 + e^-$ ($\Delta_r H^o_{298} = 16.10$ eV) is the only thermochemically open channel. It is likely that this reaction involves a tightly-constrained transition state and a barrier in the exit channel. It is then possible to explain the lack of correspondence between $AE_{298}(CF_2-CH_2^+)$ and the energy of the dissociation channel $CF_2-CH_2^+ + F_2 + e^-$. The yield of $CF^+$ is very weak, and the $AE_{298}$ can only be bracketed between 21 and 23 eV. No

attempt is made to identify the accompanying neutral fragments. We note that $CF^+$ is also observed from dissociative photoionisation of $CH_2F_2$ for photon energies above 20 eV.[34]

### 4.2.2 Coincidence ion yields of $CHF_2-CHF_2{}^+$

The dissociative photoionisation of $CHF_2-CHF_2$ has some similarities, but significant differences from that of $CF_3-CH_2F$. In part, the differences can be explained by the different symmetries of the two isomers. First, we consider the major ions. For the low-energy parts of the Franck-Condon region of the ground state of $CHF_2-CHF_2{}^+$, the parent ion is observed weakly with a branching ratio of unity. In the range 12.18 to 12.57 eV, TPEPICO-TOF spectra of this ion have Gaussian peakshapes with fwhm approximately equal to 180 ns, similar to that observed for the 1,1,1,2 isomer. At higher energies within the ground state, the parent ion signal decreases and $CHF_2{}^+$ is observed with an $AE_{298}$ of $12.57 \pm 0.05$ eV, corresponding to $\Delta_r H^o{}_{298}$ for $CHF_2-CHF_2 \rightarrow CHF_2{}^+ + CHF_2 + e^-$ of $12.73 \pm 0.05$ eV.[26] At the Franck-Condon maximum of 13.00 eV, this fragment ion has a relative yield of unity. Because of symmetry, cleavage of the C–C bond by dissociative photoionisation can only produce $CHF_2{}^+$. This value for $\Delta_r H^o{}_{298}$ is used to determine $\Delta_f H^o{}_{298}(CHF_2-CHF_2)$ to be $-861 \pm 5$ kJ mol$^{-1}$. From the measured onset of ionisation, 12.18 eV, we also determine $\Delta_f H^o{}_{298}(CHF_2-CHF_2{}^+) \leq 314$ kJ mol$^{-1}$; the G2 calculation yields an absolute value of 233 kJ mol$^{-1}$.

At the onset of the first excited state of $CHF_2-CHF_2{}^+$, 14.4 eV, the threshold photoelectron signal starts to rise, the $CHF_2{}^+$ signal falls, and two new major ions appear with TOFs of 16.06 and 17.73 μs and $AE_{298}$ values of $14.45 \pm 0.07$ and $14.38 \pm 0.07$ eV, respectively. The former ion has exactly the same TOF as that caused by F-atom loss from $CF_3-CH_2F^+$ (see above). It therefore has a mass of 83 u, and is due to $CHF-CHF_2{}^+$; a structure involving rearrangement, such as $CH_2-CF_3{}^+$, seems very unlikely. The TOF of the latter ion is slightly but significantly different from that of the parent ion, 17.81 μs, and is due to H-atom loss to form $CF_2-CHF_2{}^+$. At 14.9 eV, corresponding to a shoulder in the TPES and probable formation of $CHF_2-CHF_2{}^+$ $\widetilde{A}$ $^2B_u$, the relative yields of $CHF-CHF_2{}^+$ and $CF_2-CHF_2{}^+$ are similar, whereas at 15.7 eV, the most intense peak in the TPES and probably due to formation of $CHF_2-CHF_2{}^+$ $\widetilde{B}$ $^2A_g$, the relative yield of the former ion is dominant at *ca.* 0.6 (Fig. 6). As with the 1,1,1,2 isomer, it seems likely that these two ions are produced directly from the $\widetilde{A}$ and $\widetilde{B}$ states of $CHF_2-CHF_2{}^+$ by cleavage of either a C–F or C–H bond. Using the $AE_{298}$ for $CF_2-CHF_2{}^+$ of $14.38 \pm 0.07$ eV corresponding to an upper limit of $\Delta_r H^o{}_{298}$ for the reaction $CHF_2-CHF_2 \rightarrow CF_2-CHF_2{}^+ + H + e^-$ to be $14.54 \pm 0.07$ eV,[26] we determine $\Delta_f H^o{}_{298}(CF_2-CHF_2{}^+) \leq 324$ kJ mol$^{-1}$. There is no literature value for this ion, so it is not possible to calculate an independent value of $\Delta_r H^o{}_{298}$ for this reaction. We show later that the dissociation $CHF_2-CHF_2{}^+ \rightarrow CF_2-CHF_2{}^+ + H$ has a considerable kinetic energy release, so it is possible that the true enthalpy of formation of this ion may be significantly lower. A G2 calculation gives

$\Delta_f H°_{298}(CF_2-CHF_2^+) = 174$ kJ mol$^{-1}$. Using the $AE_{298}$ of CHF–CHF$_2^+$ of $14.45 \pm 0.07$ eV, corresponding to an upper limit of $\Delta_r H°_{298}$ for the reaction CHF$_2$–CHF$_2$ $\rightarrow$ CHF–CHF$_2^+$ + F + e$^-$ to be $14.60 \pm 0.07$ eV, we determine $\Delta_f H°_{298}$(CHF–CHF$_2^+$) $\leq 469$ kJ mol$^{-1}$. The G2 calculation gives $\Delta_f H°_{298}$(CHF–CHF$_2^+$) = 419 kJ mol$^{-1}$. Both values can be compared with a literature value of 332 kJ mol$^{-1}$,[29] determined from the proton affinity of CHF=CF$_2$. The main difference in the fragmentation of CHF$_2$–CHF$_2^+$ compared to CF$_3$–CH$_2$F$^+$ over this range of *ca.* 14-17 eV is the observation of C–H bond fission in the former, but not in the latter isomer. This may relate to the differences in the energetics of the dissociation channels. Whereas for the 1,1,1,2 isomer reactions involving C–H and C–F fission are almost iso-energetic (Section 4.2.1), with the 1,1,2,2 isomer the reaction to CF$_2$–CHF$_2^+$ + H + e$^-$ (13.45 eV) is calculated by the G2 method to be over 1 eV less endothermic than to CHF–CHF$_2^+$ + F + e$^-$ (14.54 eV). Thus at the onset of the $\widetilde{A}$ state of CHF$_2$–CHF$_2^+$, 14.4 eV, the channel involving C–F bond fission is closed, whilst that involving C–H fission is open.

Above 16.5 eV the relative yield of both CF$_2$–CHF$_2^+$ and CHF–CHF$_2^+$ drops, and that of the minor ion CH$_2$F$^+$ increases. Its yield follows the TPES signal in the range 18-22 eV, with peaks in both spectra at 18.8 and 20.1 eV. In this range CH$_2$F$^+$ is the dominant ion with a branching ratio of *ca.* 0.7-1.0 (Figure 6), the remainder of the ion signal being mainly due to CHF$_2^+$. (As in the 1,1,1,2 isomer, there is some evidence for a very small contribution of CHF$^+$ to the ion yield of CH$_2$F$^+$.) Above 22 eV, CHF$_2^+$ reverts to being the dominant ion.

As with the 1,1,1,2 isomer, above 16 eV minor ions are observed with TOFs of 9.78, 10.05 and 14.05 μs. They are assigned to CF$^+$, CH$_2$F$^+$ and CHF–CHF$^+$, with the same caveat as before about the number of hdrogen atoms in all three fragments. The AEs of CH$_2$F$^+$ and CHF–CHF$^+$ are $16.48 \pm 0.07$ and $16.53 \pm 0.07$ eV, respectively. The yield of CH$_2$F$^+$ is shown in Figure 4(c). The TOF of this ion is identical to that of the major ion formed from C–C bond fission of CF$_3$–CH$_2$F$^+$ where the $AE_{298}$ is 12.99 eV. Since the $AE_{298}$(CH$_2$F$^+$) from the two isomers is so different, the signal from the 1,1,2,2 isomers must arise from photon-induced fragmentation of CHF$_2$–CHF$_2$, and therefore involves H-atom migration across the C–C bond. This situation is comparable to the production of CHF$_2^+$ from CF$_3$–CH$_2$F. The possible neutral fragments associated with CH$_2$F$^+$ from CHF$_2$–CHF$_2$ are shown in Table 2 Column 1. The most likely channel is production of CH$_2$F$^+$ with CF$_2$ + F + e$^-$, where the value of $\Delta_r H°_{298}$, 16.49 eV, is close to the observed onset of CH$_2$F$^+$. The yield of CHF–CHF$^+$ (64 u) is shown in Figure 4(b), and there is now no overlapping signal of CF$_3^+$ (69 u). As with the 1,1,1,2 isomer, the thermochemistry of the possible reaction products of the 1,1,2,2 isomer suggests that CHF–CHF$^+$ can only form with F$_2$ + e$^-$, and not with 2F + e$^-$ ; it is assumed that each carbon atom in CHF$_2$–CHF$_2$ loses one fluorine atom each. Similar to the

1,1,1,2 isomer, the yield of $CF^+$ from $CHF_2-CHF_2^+$ is very weak, and the $AE_{298}$ can only be bracketed between 20 and 23 eV. In the high-energy range of 18-22 eV, the major difference between the two isomers is that the minor ion, $CH_2F^+$, becomes the dominant fragment from dissociative photoionisation of $CHF_2-CHF_2$, whereas the major ion, also $CH_2F^+$, becomes dominant from $CF_3-CH_2F$.

## 4.3 Fixed-energy TPEPICO spectra

TPEPICO-TOF spectra at a resolution of 8 ns have been recorded for all the major fragment ions, corresponding to a single bond cleavage, at photon energies corresponding to the Franck-Condon maxima of the valence states of $CF_3-CH_2F^+$ and $CHF_2-CHF_2^+$. These measurements include the parent ion spectra, already described, where the peakshapes are Gaussian with fwhm proportional to $(MT)^{1/2}/E$, where M is the mass of the parent ion, T the temperature, and E the extraction field from the interaction region.[32,33] Fragments ions often have enough translational energy for the TOF peak to be substantially broadened from that expected for a thermal source. Analysis of the shape of such TOF peaks allows a determination of the kinetic energy release distribution (KERD), and hence the total mean translational kinetic energy release, $<KE>_T$, associated with a particular dissociation process. The thermal energy of the parent molecule at 298 K is convoluted into each component of the KERD, and the analysis can only apply to a two-body process with a single bond cleavage. (TPEPICO-TOF spectra of the minor ions were therefore not recorded.) As an example, Figure 7 shows the TPEPICO-TOF spectrum of $CF_2-CH_2F^+$ from $CF_3-CH_2F$ photoexcited at 17.1 eV. Full details of the fitting procedure are described elsewhere,[21,22] and the fit to this peak shape yields $<KE>_T = 0.95 \pm 0.02$ eV. It is found that the values of $<KE>_T$ are usually relatively insensitive to the exact form of the KERD, and the errors quoted by the fitting program are probably unrealistically low.

$<KE>_T$ can be divided by the available energy, $E_{avail}$, defined as the photon energy minus the thermochemical dissociation energy (*i.e.* $\Delta_r H^o_{298}$ in Table 2 Column 3), to determine the fraction of the available energy, $f_T$, being channelled into translational energy of the two fragments. These experimental values of $f_T$ can then be compared with those expected if the dissociation follows a purely statistical or a purely impulsive model. These models, with original source references, are described in detail in our recent work on dissociative photoionisation of $CHF_2-CF_3$ [6] and elsewhere.[35] The experimentally-determined values of $<KE>_T$ and $f_T$ are shown in Table 3, together with calculated values of $f_T$ for statistical [36] and pure-impulsive [37] dissociation models. Since many of the vibrational frequencies of the fragment ions are unknown, statistical values for $f_T$ were calculated according to the lower limit value of $1/(x+1)$, where $x$ is the number of vibrational degrees of freedom in the transition state of the unimolecular reaction.[38] For both isomers of $C_2F_4H_2^+$ with eight atoms, $x = 3N-7$ or 17, giving a

predicted statistical $f_T \geq 0.06$. If dissociation follows the modified-impulsive model,[35,39] values of $f_T$ may be greater than those calculated for the pure-impulsive model.

The results fall into two groups. The $f_T$ values for fragment ions caused by fission of the C−C bond are low, always less than 0.10. For each of the three dissociation channels studied, $<KE>_T$ increases slowly with hν. Assuming dissociation always occurs to the ground electronic states of $CH_2F^+ + CF_3$, $CF_3^+ + CH_2F$ or $CHF_2^+ + CHF_2$, $f_T$ remains approximately constant and close to the fraction predicted for statistical decay. By contrast, the $f_T$ values for fragment ions caused by fission of a terminal C−H or C−F bond are much higher ; 0.34-0.76 for loss of a fluorine atom, over unity for loss of a hydrogen atom. The absolute values of $f_T$, especially for this second group, should be treated with caution for two reasons. First, they depend upon the values used for $E_{avail}$, which themselves depend on a precise knowledge of $\Delta_r H^o_{298}$ for the reaction. For F- and H-atom loss from both $CF_3$−$CH_2F^+$ and $CHF_2$−$CHF_2^+$, these values are not known ; we can only use the $AE_{298}$ of the fragment ion, corrected for thermal effects,[26] which, by definition, is an upper limit to the true dissociation energy. Thus for these processes, the $f_T$ values can only be an upper limit. Second, the result for H-atom loss from $CHF_2$−$CHF_2$ photoexcited at 14.94 eV, $f_T$ = 2.2, is anomalous. In part, this high value may arise because of the unfavourable kinematics of the dissociation. Since the daughter ion, $CF_2$−$CHF_2^+$, carries away less than 1 % of the total kinetic energy, any error in the determination of the KE of the daughter ion is magnified hugely in obtaining the value of $<KE>_T$. Nevertheless, all these values of $f_T$ for F- or H-atom loss are closer to the predictions of the impulsive than those of the statistical model. These observations are consistent with the arguments presented in Section 3 that the $\widetilde{A}$ and $\widetilde{B}$ states of the parent ion, produced by electron removal from either a C−H σ-bonding orbital or a F 2pπ lone-pair orbital, show isolated-state behaviour. That is, dissociation proceeds along a pseudo-diatomic exit channel of the potential energy surface of the particular electronic state photoexcited. The two atoms of the bond that breaks recoil with such force that dissociation results in a relatively large fraction of the available energy being channelled into translational energy of the fragments. This is the same behaviour as observed for $CF_3$−$CF_3^+$ [4,24,25] and $CHF_2$−$CF_3^+$,[6] where F-atom loss is observed with a high branching ratio over a narrow region of energy corresponding to the Franck-Condon region of one or two excited valence states of the parent ion.

## 5. DISCUSSION

### 5.1 F- and H-atom loss from $CF_3$−$CH_2F^+$ and $CHF_2$−$CHF_2^+$

The loss of a fluorine or hydrogen atom from both isomers of $C_2F_4H_2^+$ is associated with isolated-state behaviour of the first or second excited electronic state of the parent ion, and direct impulsive dissociation off a potential energy surface which is probably repulsive along the reaction coordinate. Under these circumstances the $AE_{298}$ of the fragment ion, even after correction for the internal energy of the ion at 298

15

K,[26] can be significantly greater than the thermochemical energy of the dissociation channel, $\Delta_r H^o_{298}$. It is therefore only possible to determine upper limits to $\Delta_f H^o_{298}$ of such fragment ions ;

$\Delta_f H^o_{298}(CF_2-CH_2F^+) \leq 485 \pm 7$, $\Delta_f H^o_{298}(CF_2-CHF_2^+) \leq 324 \pm 7$ and $\Delta_f H^o_{298}(CHF-CHF_2^+) \leq 469 \pm 7$ kJ mol$^{-1}$. G2 calculations for these three ions give 330, 174 and 419 kJ mol$^{-1}$, respectively, consistent with our data. The only other experimental data with which to compare these values is for $CHF-CHF_2^+$, where a value of 332 kJ mol$^{-1}$ has been determined indirectly [29] from the proton affinity of $CHF=CF_2$.

Recently, we have described a method to determine the dissociative ionisation energy of polyatomic molecules whose ground state of the parent ion is repulsive ; indirectly, this is a means to determine *absolute* enthalpies of formation of radical cations.[40] Briefly, TPEPICO spectra at high time resolution are measured as a function of photon energy over the Franck-Condon region of the repulsive state of the parent cation. By determining $<KE>_T$ as a function of hv, a linear extrapolation can be performed to determine the photon energy at which $<KE>_T$ would be zero. This quantity is termed the dissociative ionisation energy of the molecule, from which the absolute enthalpy of formation of the fragment ion can be determined. We applied this technique to dissociation from the repulsive electronic ground states of $CF_4^+$ (to $CF_3^+$ + F), $SF_6^+$ (to $SF_5^+$ + F) and $CF_3SF_5^+$ (to $CF_3^+$ + $SF_5$),[40] and obtained values for the enthalpies of formation of $CF_3^+$ and $SF_5^+$ in good agreement with other methods. We have attempted to apply this method here to dissociative *excited* states of parent cations, in particular $CF_3-CH_2F^+$ $\widetilde{A}$ and $\widetilde{B}$ (to $CF_2-CH_2F^+$ + F). The results, however, were inconclusive, and we were not able to extrapolate satisfactorily the graphs of $<KE>_T$ *vs.* hv to $<KE>_T = 0$. This very challenging experiment was not attempted for F- or H-atom loss from either the $\widetilde{A}$ or $\widetilde{B}$ states of $CHF_2-CHF_2^+$. It is hoped that future experiments will yield definitive values for the enthalpies of formation of such cations.

## 5.2 Kinetic energy releases

The large values of $f_T$ observed for fission of a C−F or C−H bond from either isomer of $C_2F_4H_2^+$ have been discussed in Section 4.3. The consequences of these values for the thermochemistry of reaction channels producing $CF_2-CH_2F^+$, $CF_2-CHF_2^+$ and $CHF-CHF_2^+$ are discussed in Section 5.1. One consequence of the pure-impulsive interfragment model,[38] which appears to describe F- and H-atom loss from $C_2F_4H_2^+$ reasonably well, is that the geometry of the daughter ion is likely to be similar to the corresponding moiety in the parent ion.

Here, we discuss the much smaller values of $f_T$, < 0.1, which are observed for fission of the C−C bond in $CF_3-CH_2F^+$ and $CHF_2-CHF_2^+$. There are two interpretations of these values. First, since the ground electronic state of both parent ions are bound in some parts of their potential energy surface, it is possible that such dissociations occur by internal conversion from the initially-excited state to high vibrational

levels of the ground state, followed by statistical dissociation from that potential energy surface. Second, Mitchell and Simons [41] have shown that impulsive dissociation can cause a much lower value of $f_T$ than the interfragment impulsive models described in Section 4.3 suggest, if one of the bond lengths or bond angles in the fragment ion is significantly different from its value in the parent ion. This is possible for $CF_3^+$, $CH_2F^+$ and $CHF_2^+$, since all three groups are approximately pyramidal when located in the parent ion but planar in the isolated ion. As the C−C bond breaks, there could then be a large change in the degree of planarity of both receding fragments in the impulsive fragmentation, with significant energy being deposited in the $\nu_2$ umbrella vibrational mode of both fragment ion and fragment neutral. We believe that the statistial mechanism, following internal conversion to high vibrational levels of the ground state, seems more likely for the lower-lying electronic states of $CF_3–CH_2F^+$ and $CHF_2–CHF_2^+$. For the higher-lying states above *ca.* 18 eV, however, it is not possible to determine the mechanism of dissociation, since both models described above could lead to low values of $f_T$.

## 6. CONCLUSIONS

Using tunable vacuum-UV radiation from a synchrotron, we have recorded the threshold photoelectron and TPEPICO spectra of $CF_3–CH_2F$ and $CHF_2–CHF_2$ over the energy range 12-25 eV. Ion yield curves and breakdown diagrams have been determined. The mean translational kinetic energy releases into the dissociation products involving a single bond cleavage from $(CF_3–CH_2F^+)^*$ and $(CHF_2–CHF_2^+)^*$ have been measured, and compared with the predictions of statistical and pure-impulsive mechanisms. *Ab initio* G2 calculations have determined the minimum-energy geometries of $CF_3–CH_2F$ and $CHF_2–CHF_2$ and their cations, and deduced the nature of the high-lying valence orbitals of both neutral molecules. Furthermore, enthalpies of formation at 298 K of both neutral molecules, and all the neutral and fragment ions observed by dissociative photoionisation have been calculated.

Combining experimental and theoretical data, the decay mechanism of the ground and first two excited valence states of $CF_3–CH_2F^+$ and $CHF_2–CHF_2^+$ have been discussed. Decay from the first and second excited states of $CF_3–CH_2F^+$ occurs impulsively by C−F bond fission to $CF_2–CH_2F^+$ (or $CF_3–CH_2^+$) + F, with a large fraction of the available energy, $f_T$, channeled into translational energy of the products. The geometry of the daughter ion is not significantly different from that of the corresponding group in $CF_3–CH_2F^+$. Decay from the analogous states of $CHF_2–CHF_2^+$ occurs by both C−H and C−F bond fission to $CF_2–CHF_2^+$ + H and $CHF–CHF_2^+$ + F respectively, again with large values of $f_T$. By contrast, the ground and higher-lying states of both $CF_3–CH_2F^+$ and $CHF_2–CHF_2^+$ dissociate by C−C bond fission to $CH_2F^+$ + $CF_3$ and $CF_3^+$ + $CH_2F$, and $CHF_2^+$ + $CHF_2$, respectively. With $CF_3–CH_2F$, $CH_2F^+$ is the dominant ion. The values for $f_T$ are now much lower, and it is not possible to deduce unambiguously the mechanism of the C−C bond cleavage.

Several examples of minor fragment ions caused by more complicated unimolecular reactions involving H- or F-atom migration across the central C−C bond are observed.  Indeed, for $h\nu > 18$ eV, $CH_2F^+$ is the dominant fragment ion from dissociative photoionisation of $CHF_2$−$CHF_2$.  New experimental values are determined for the enthalpy of formation at 298 K of $CF_3$−$CH_2F$, $CHF_2$−$CHF_2$, $CF_2$−$CH_2F^+$, $CF_2$−$CHF_2^+$ and $CHF$−$CHF_2^+$.

**References**

1.    R. E. Banks,  *J. Fluorine Chem.,* 1994,  **67**, 193.

2.    B. Sukornick,  *Int. J. Thermophys.,* 1989, **10**, 553.

3.    A. R. Ravishankara and E. R. Loveday,
        *J. Chem. Soc. Faraday Trans.,* 1994, **90**, 2159.

4.    G. K. Jarvis, K. J. Boyle, C. A. Mayhew and R. P. Tuckett,
        *J. Phys. Chem. A.,* 1998, **102**, 3219.

5.    G. K. Jarvis, K. J. Boyle, C. A. Mayhew and R. P. Tuckett,
        *J. Phys. Chem. A.,* 1998, **102**, 3230.

6.    Weidong Zhou, D. P. Seccombe, R. P. Tuckett and M. K. Thomas,
        *Chem. Phys.,*  2002  in press.

7.    Weidong Zhou, D. P. Seccombe, R. Y. L. Chim and R. P. Tuckett,
        *Surface Review and Letters,* 2002,  **9**, xxxx.

8.    T. Ogata and Y. Miki,  *J. Mol. Struct.,* 1986, **140**, 49.

9.    D. E. Brown and B. Beagley,  *J. Mol. Struct.,* 1977, **38**, 167.

10.   G. N. B. al-Ajdah, B. Beagley and M. O. Jones,
        *J. Mol. Struct.,* 1980, **65**, 271.

11.   D. McNaughton, C. Evans and E. G. Robertson,
        *J. Chem. Soc. Faraday Trans.,* 1995, **91**, 1723.

12.   R. D. Parra and X. C. Zeng, *J. Phys. Chem. A.,* 1998, **102**, 654.

13. S. Papasavva, S. Tai, A. Esslinger, K. H. Illinger and J. E. Kenny,
    *J. Phys. Chem.,* 1995, **99**, 3438.

14. S. Papasavva, K. H. Illinger and J. E. Kenny, *J. Phys. Chem.,* 1996, **100**, 10100.

15. Y Chen, S. J. Paddison and E. Tschuikow-Roux, *J. Phys. Chem.,* 1994, **98**, 1100.

16. S. S. Chen, A. S. Rodgers, J. Chao, R. C. Wilhoit and B. J. Zwolinski,
    *J. Phys. Chem. Ref. Data,* 1975, **4**, 441.

17. L. A. Curtiss, K. Raghavachari, G. W. Trucks and J. A. Pople,
    *J. Chem. Phys.,* 1991, **94**, 7221.

18. P. A. Hatherly, M. Stankiewicz, K. Codling, J. C. Creasey, H. M. Jones and R. P. Tuckett,
    *Meas. Sci. Technol.,* 1992, **3**, 891.

19. P. A. Hatherly, D. M. Smith and R. P. Tuckett, *Zeit. Phys. Chem.,* 1996, **195**, 97.

20. W. C. Wiley and I. H Maclaren, *Rev. Sci. Instr.,* 1955, **26**, 1150.

21. I. Powis, P. I. Mansell and C. J. Danby, *Int. J. Mass Spectrom. Ion Phys.,* 1979, **32**, 15.

22. G. K. Jarvis, D. P. Seccombe and R. P. Tuckett, *Chem. Phys. Lett.,* 1999, **315**, 287.

23. M. Horn, M. Oswald, R. Oswald and P. Botschwina,
    *Ber. Buns. Phys. Chem.,* 1995, **99**, 323.

24. M. G. Inghram, G. R. Hanson and R. Stockbauer,
    *Int. J. Mass Spec. Ion Phys.,* 1974, **14**, 285.

25. I. G. Simm, C. J. Danby, J. H. D. Eland and P. I. Mansell,
    *J. Chem. Soc. Farad. Trans. 2.,* 1976, **72**, 426.

26. J C Traeger and R G McLoughlin, *J. Amer. Chem. Soc.,* 1981, **103**, 3647.

27. G K Jarvis and R P Tuckett, *Chem. Phys. Letts.,* 1998, **295**, 145.

28. M. W. Chase, *J. Phys. Chem. Ref. Data,* 1998, Monograph No. 9.

29. S. G. Lias, J. E. Bartmess, J. F. Liebman, J. L. Holmes, R. D. Levin and W. G. Mallard,
    *J. Phys. Chem. Ref. Data,* 1988, **17**, Supplement No. 1.

30. B. Ruscic, J. V. Michael, P. C. Redfern, L. A. Curtiss and K. Raghavachari,
    *J. Phys. Chem. A.,* 1998, **102**, 10889.

31. G. A. Garcia, P. M. Guyon and I. Powis, *J. Phys. Chem. A.,* 2001, **105**, 8296.

32. J. L. Franklin, P. M. Hierl and D. A. Whan, *J. Chem. Phys.,* 1967, **47**, 3148.

33. J. H. D. Eland, *Int. J. Mass Spectrom. Ion Phys.,* 1972, **8**, 143.

34. D. P. Seccombe, R. P. Tuckett and B. O. Fisher, *J. Chem. Phys.,* 2001, **114**, 4074.

35. D. P. Seccombe, R. Y. L. Chim, G. K. Jarvis and R. P. Tuckett,

*Phys. Chem. Chem. Phys.,* 2000, **2**, 769.

36.     C. E. Klots, *J. Chem. Phys.,* 1973, **58**, 5364.

37.     K. E. Holdy, L. C. Klots and K. R. Wilson, *J. Chem. Phys.,* 1970, **52**, 4588.

38.     J. L. Franklin, *Science,* 1976, **193**, 725.

39.     G. E. Busch and K. R. Wilson, *J. Chem. Phys.,* 1972, **56**, 3626.

40.     R. Y. L. Chim, R. A. Kennedy, R. P. Tuckett, W. Zhou, G. K. Jarvis, D. J. Collins and P. A. Hatherly, *J. Phys. Chem. A.,* 2001, **105**, 8403.

41.     R. C. Mitchell and J. P. Simons, *Disc. Faraday Soc.,* 1967, **44**, 208.

**Table 1.** Calculated minimum energy geometries for the ground electronic state of neutral and parent cation of $CF_3-CH_2F$ and $CHF_2-CHF_2$.

| Species | $CF_3-CH_2F$ | $CF_3-CH_2F^+$ | Species | $CHF_2-CHF_2$ | $CHF_2-CHF_2^+$ |
|---|---|---|---|---|---|
| Symmetry | $C_s$ | $C_s$ | Symmetry | $C_{2h}$ | $C_{2h}$ |
| Electronic state | $\widetilde{X}\ {}^1A'$ | $\widetilde{X}\ {}^2A'$ | Electronic state | $\widetilde{X}\ {}^1A_g$ | $\widetilde{X}\ {}^2A_g$ |
| R (C1, C2) | 1.5065 | 1.9394 | R (C1, C2) | 1.5108 | 1.9482 |
| R (C1, F1) | 1.3519 | 1.2917 | R (C1, H1) | 1.0917 | 1.0949 |
| R (C1, F2) | 1.3443 | 1.2887 | R (C1, F1) | 1.3624 | 1.2925 |
| R (C1, F3) | 1.3443 | 1.2887 | R (C1, F2) | 1.3624 | 1.2925 |
| R (C2, F4) | 1.382 | 1.2995 | R (C2, F3) | 1.3624 | 1.2925 |
| R (C2, H1) | 1.0917 | 1.091 | R (C2, F4) | 1.3624 | 1.2925 |
| R (C2, H2) | 1.0917 | 1.091 | R (C2, H2) | 1.0917 | 1.0949 |
| ∠ C2C1F1 | 109.10 | 101.23 | ∠ C2C1H1 | 112.17 | 98.32 |
| ∠ C2C1F2 | 111.57 | 102.41 | ∠ C2C1F1 | 108.20 | 102.22 |
| ∠ C2C1F3 | 111.57 | 102.41 | ∠ C2C1F2 | 108.20 | 102.22 |
| ∠ F1C1F2 | 108.23 | 115.83 | ∠ HC1F1 | 109.72 | 117.30 |
| ∠ F1C1F3 | 108.23 | 115.83 | ∠ HC1F2 | 109.72 | 117.30 |
| ∠ F2C1F3 | 108.03 | 115.69 | ∠ F1C1F2 | 108.75 | 114.92 |
| ∠ C1C2F4 | 108.45 | 102.51 | ∠ C1C2F3 | 108.20 | 102.22 |
| ∠ C1C2H1 | 109.08 | 97.98 | ∠ C1C2F4 | 108.20 | 102.22 |
| ∠ C1C2H2 | 109.08 | 97.98 | ∠ C1C2H2 | 112.17 | 98.32 |
| ∠ F4C2H1 | 109.89 | 114.91 | ∠ F3C2F4 | 108.75 | 114.92 |
| ∠ F4C2H2 | 109.89 | 114.91 | ∠ F3C2H2 | 10972 | 117.30 |
| ∠ H1C2H2 | 110.42 | 122.28 | ∠ F4C2H2 | 109.72 | 117.30 |
| D (F1C1C2F4) | 180.0 | 180.0 | D(H1C1C2F3) | 58.84 | 59.61 |
| D(F1C1C2H1) | -60.34 | -62.17 | D(H1C1C2F4) | -58.83 | -59.61 |
| D(F1C1C2H2) | 60.34 | 62.17 | D(H1C1C2H2) | -180.0 | -180.0 |
| D(F2C1C2F4) | -60.47 | -60.10 | D(F1C1C2F3) | -180.0 | -180.0 |
| D(F2C1C2H1) | 59.19 | 57.73 | D(F1C1C2F4) | 62.33 | 60.79 |
| D(F2C1C2H2) | 179.87 | -177.92 | D(F1C1C2H2) | -58.83 | -59.61 |
| D(F3C1C2F4) | 60.47 | 60.10 | D(F2C1C2F3) | -62.33 | -60.79 |
| D(F3C1C2H1) | -179.87 | 177.92 | D(F2C1C2F4) | -180.0 | -180.0 |
| D(F3C1C2H2) | -59.19 | -57.73 | D(F2C1C2H2) | 58.84 | 59.61 |
| $E_0$ / Hartree | -476.275554 | -475.825496 | $E_0$ / Hartree | -476.265111 | -475.832594 |
| Adiabatic IE / eV | 12.25 | | Adiabatic IE / eV | 11.77 | |

**Table 2**.   Energetics of dissociative photoionisation pathways of $CF_3-CH_2F$ and $CHF_2-CHF_2$.

_____

Major [a] ion products of $CF_3-CH_2F$ (-905)

|  | $AE_{298}$ / eV | $\Delta_rH^o{}_{298}$ / eV [c] | G2 / eV [d] |
|---|---|---|---|
| $CF_3-CH_2F^+$ + e⁻ | 12.64 (5) |  | 12.25 |
| $CH_2F^+$ (+833) + $CF_3$ (-466) + e⁻ | 12.99 (5) | 13.15 (5) | 13.32 |
| $CF_3{}^+$ (+406) + $CH_2F$ (-33) + e⁻ | 13.12 (5) | 13.29 (5) | 13.38 |
| $CF_2-CH_2F^+$ (unknown)[e] + F (+79) + e⁻ | 15.07 (7) | 15.23 (7) | 13.90 |

Minor [b] ion products of $CF_3-CH_2F$ (-905)

| | | |
|---|---|---|
| $CHF_2{}^+$ (+604)  + $CHF_2$ (-237) + e⁻ | 16.11 (7) | 13.18 |
| + CF (+255) + HF (-272) + e⁻ | | 15.46 |
| + $CF_2$ (-182) + H (+218) + e⁻ | | 16.01 |
| + CHF (+125) + F (+79) + e⁻ | | 17.76 |
| + CH (+596) + $F_2$ (0) + e⁻ | | 21.82 |
| | | |
| $CF_2-CH_2{}^+$ (+648)      + $F_2$ (0) + e⁻ | 16.57 (7) | 16.10 |
| + 2F (+158) + e⁻ | | 17.73 |
| | | |
| $CF^+$ (+1149)         + neutrals + e⁻ | 21.0-23.0 | ?? |

_____

Major [a] ion products of $CHF_2-CHF_2$ (-861)

|  | $AE_{298}$ / eV | $\Delta_rH^o{}_{298}$ / eV | G2 / eV |
|---|---|---|---|
| $CHF_2-CHF_2{}^+$ + e⁻ | 12.18 (5) |  | 11.77 |
| $CHF_2{}^+$ (+604) + $CHF_2$ (-237) + e⁻ | 12.57 (5) | 12.73 (5) | 12.84 |
| $CF_2-CHF_2{}^+$ (unknown)[f] + H (+218) + e⁻ | 14.38 (7) | 14.54 (7) | 13.45 |
| $CHF-CHF_2{}^+$ (unknown)[g] + F (+79) + e⁻ | 14.45 (7) | 14.60 (7) | 14.54 |

Minor [b] ion products of $CHF_2-CHF_2$ (-861)

| | | |
|---|---|---|
| $CH_2F^+$ (+833)  + $CF_3$ (-466) + e⁻ | 16.48 (7) | 12.73 |

|  |  |  |  |
|---|---|---|---|
| | + $CF_2$ (-182) + F (+79) + $e^-$ | | 16.49 |
| | + CF (+255) + $F_2$ (0) + $e^-$ | | 20.20 |
| | | | |
| $CHF-CHF^+$ (+690) | + $F_2$ (0) + $e^-$ | 16.53 (7) | 16.08 |
| | + 2F (+158) + $e^-$ | | 17.71 |
| | | | |
| $CF^+$ (+1149) | + neutrals + $e^-$ | 20.0-23.0 | ?? |

---

[a]  Major ion product is defined as either the parent ion, or a fragment ion caused by a single bond fission.

[b]  Minor ion product is defined as a fragment ion caused by fission of multiple bonds.

[c]  For the major ions, the value of $\Delta_r H^o{}_{298}$ is derived from $AE_{298}$ of the fragment ion using the procedure of Traeger and McLoughlin.[26]  For the minor ions, the value of $\Delta_r H^o{}_{298}$ is given by the enthalpy of formation of products minus that of reactants, using values for $\Delta_f H^o{}_{298}$ given in brackets in Column 1 in units of kJ mol$^{-1}$.

[d]  Enthalpy of reaction at 298 K, using enthalpies of formation of products and reactants, calculated at the G2 level of theory with optimised minimum-energy geometries.

[e]  Our data yields an upper limit for $\Delta_f H^o{}_{298}(CF_2-CH_2F^+)$ of $485 \pm 7$ kJ mol$^{-1}$.

[f]  Our data yields an upper limit for $\Delta_f H^o{}_{298}(CF_2-CHF_2{}^+)$ of $324 \pm 7$ kJ mol$^{-1}$.

[g]  Our data yields an upper limit for $\Delta_f H^o{}_{298}(CHF-CHF_2{}^+)$ of $469 \pm 7$ kJ mol$^{-1}$.

**Table 3.** Mean translation KE releases, $\langle KE \rangle_T$, of the two-body fragmentation of the valence states of $CF_3-CH_2F^+$ and $CHF_2-CHF_2^+$.

| Parent Ion | Fragment Ion | hν / eV | $E_{avail}$ / eV [a] | $\langle KE \rangle_T$ / eV | **Fraction Ratio** [b] *Expimental* | **Fraction Ratio** *Statistical* | Fraction Ratio *Impulsive* |
|---|---|---|---|---|---|---|---|
| $CF_3-CH_2F^+$ | $CH_2F^+$ | 13.93 | 0.78 | $0.01 \pm 0.002$ | 0.01 | 0.06 | 0.27 |
| | | 16.42 | 3.27 | $0.24 \pm 0.01$ | 0.07 | 0.06 | 0.27 |
| | | 17.10 | 3.95 | $0.27 \pm 0.01$ | 0.07 | 0.06 | 0.27 |
| | | 18.02 | 4.87 | $0.16 \pm 0.01$ | 0.03 | 0.06 | 0.27 |
| | | 20.00 | 6.85 | $0.35 \pm 0.01$ | 0.05 | 0.06 | 0.27 |
| | | 20.66 | 7.51 | $0.43 \pm 0.02$ | 0.06 | 0.06 | 0.27 |
| | | 23.05 | 9.90 | $0.70 \pm 0.03$ | 0.07 | 0.06 | 0.27 |
| | $CF_3^+$ | 13.93 | 0.64 | $0.02 \pm 0.002$ | 0.03 | 0.06 | 0.27 |
| | | 16.42 | 3.13 | $0.15 \pm 0.01$ | 0.05 | 0.06 | 0.27 |
| | | 17.10 | 3.81 | $0.30 \pm 0.01$ | 0.08 | 0.06 | 0.27 |
| | | 18.02 | 4.73 | $0.32 \pm 0.01$ | 0.07 | 0.06 | 0.27 |
| | | 20.66 | 7.37 | $0.50 \pm 0.02$ | 0.07 | 0.06 | 0.27 |
| | | 23.05 | 9.76 | $0.55 \pm 0.02$ | 0.06 | 0.06 | 0.27 |
| | $CF_2-CH_2F^+$ | 16.42 | 1.19 | $0.91 \pm 0.01$ | 0.76 | 0.06 | 0.48 |
| | | 17.10 | 1.87 | $0.95 \pm 0.02$ | 0.51 | 0.06 | 0.48 |
| | | 18.02 | 2.79 | $1.44 \pm 0.04$ | 0.52 | 0.06 | 0.48 |
| $CHF_2-CHF_2^+$ | $CHF_2^+$ | 12.92 | 0.19 | *c* | | 0.06 | 0.24 |
| | | 15.69 | 2.96 | $0.19 \pm 0.01$ | 0.06 | 0.06 | 0.24 |
| | | 17.10 | 4.37 | $0.20 \pm 0.01$ | 0.05 | 0.06 | 0.24 |
| | | 18.84 | 6.11 | $0.26 \pm 0.02$ | 0.04 | 0.06 | 0.24 |
| | | 20.00 | 7.27 | $0.34 \pm 0.01$ | 0.05 | 0.06 | 0.24 |
| | | 22.88 | 10.15 | $0.53 \pm 0.01$ | 0.05 | 0.06 | 0.24 |
| | $CF_2-CHF_2^+$ | 14.94 | 0.40 | $0.88 \pm 0.09$ | 2.20 | 0.06 | 0.93 |
| | $CHF-CHF_2^+$ | 15.69 | 1.09 | $0.58 \pm 0.03$ | 0.53 | 0.06 | 0.48 |
| | | 17.10 | 2.50 | $0.86 \pm 0.05$ | 0.34 | 0.06 | 0.48 |

[a]  $E_{avail} = h\nu - AE_{298}$ of fragment ion corrected for thermal effects by the procedure of Traeger and McLoughlin.[26]

[b]  Given by $\langle KE \rangle_T / E_{avail}$

[c]  Too small to measure.  Fit not robust to values chosen for $\Delta E_{min}$ and $n$.[23]

## Figure Captions

*Figure 1*. Computed minimum energy structure of $CF_3$–$CH_2F$ $\widetilde{X}$ $^1A'$, and its three highest valence molecular orbitals. The orbitals are calculated at the MP2/6-31(d) level of theory.

*Figure 2*. Computed minimum energy structure of $CHF_2$–$CHF_2$ $\widetilde{X}$ $^1A_g$, and its three highest valence molecular orbitals. The orbitals are calculated at the MP2/6-31(d) level of theory.

*Figure 3*. (a) Threshold photoelectron spectrum of $CF_3$–$CH_2F$. (b) and (c) Coincidence ion yields over the same energy range. The optical resolution is 0.3 nm.

*Figure 4*. (a) Threshold photoelectron spectrum of $CHF_2$–$CHF_2$. (b) and (c) Coincidence ion yields over the same energy range. The optical resolution is 0.3 nm.

*Figure 5*. Breakdown diagram for dissociative photoionisation of $CF_3$–$CH_2F$.

*Figure 6*. Breakdown diagram for dissociative photoionisation of $CHF_2$–$CHF_2$.

*Figure 7*. Coincidence TOF spectrum (dots) of $CF_2$–$CH_2F^+$ from $CF_3$–$CH_2F$ photoionised at 17.1 eV. The solid line gives the best fit to the data, comprised of five contribution (n=1,2,3,4,5) in the basis set for $\varepsilon_t(n)$.[22] The reduced probability of each contribution is shown in (b). The fit yields a total mean translational kinetic energy, $\langle KE \rangle_T$, into $CF_2$–$CH_2F^+$ + F of $0.95 \pm 0.02$ eV which constitutes 51% of the available energy.
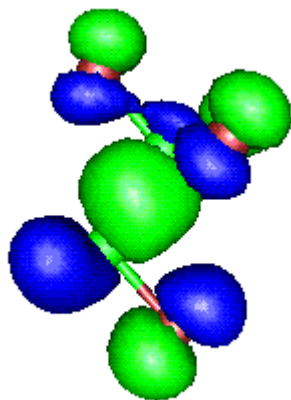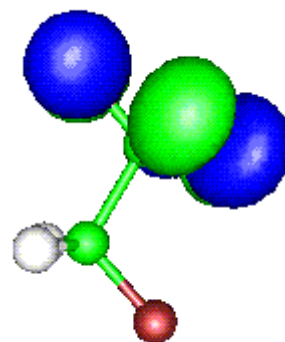
**Figure 1**
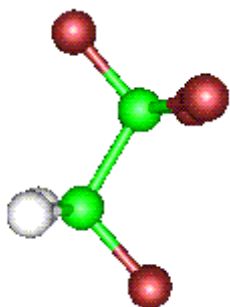


Structure of neutral
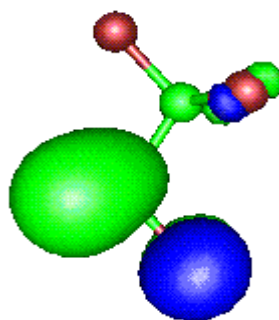
8a" (*i.e.* HOMO-1)

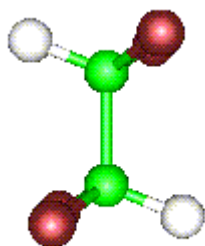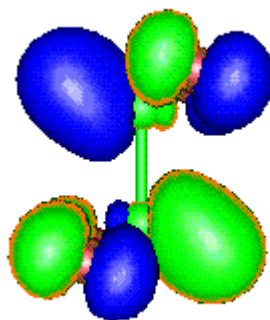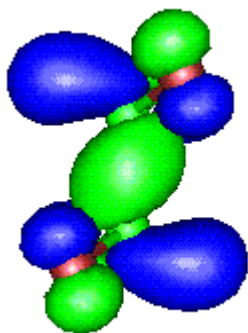17a' (*i.e.* HOMO)
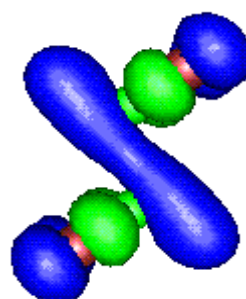
7a" (*i.e.* HOMO-2)

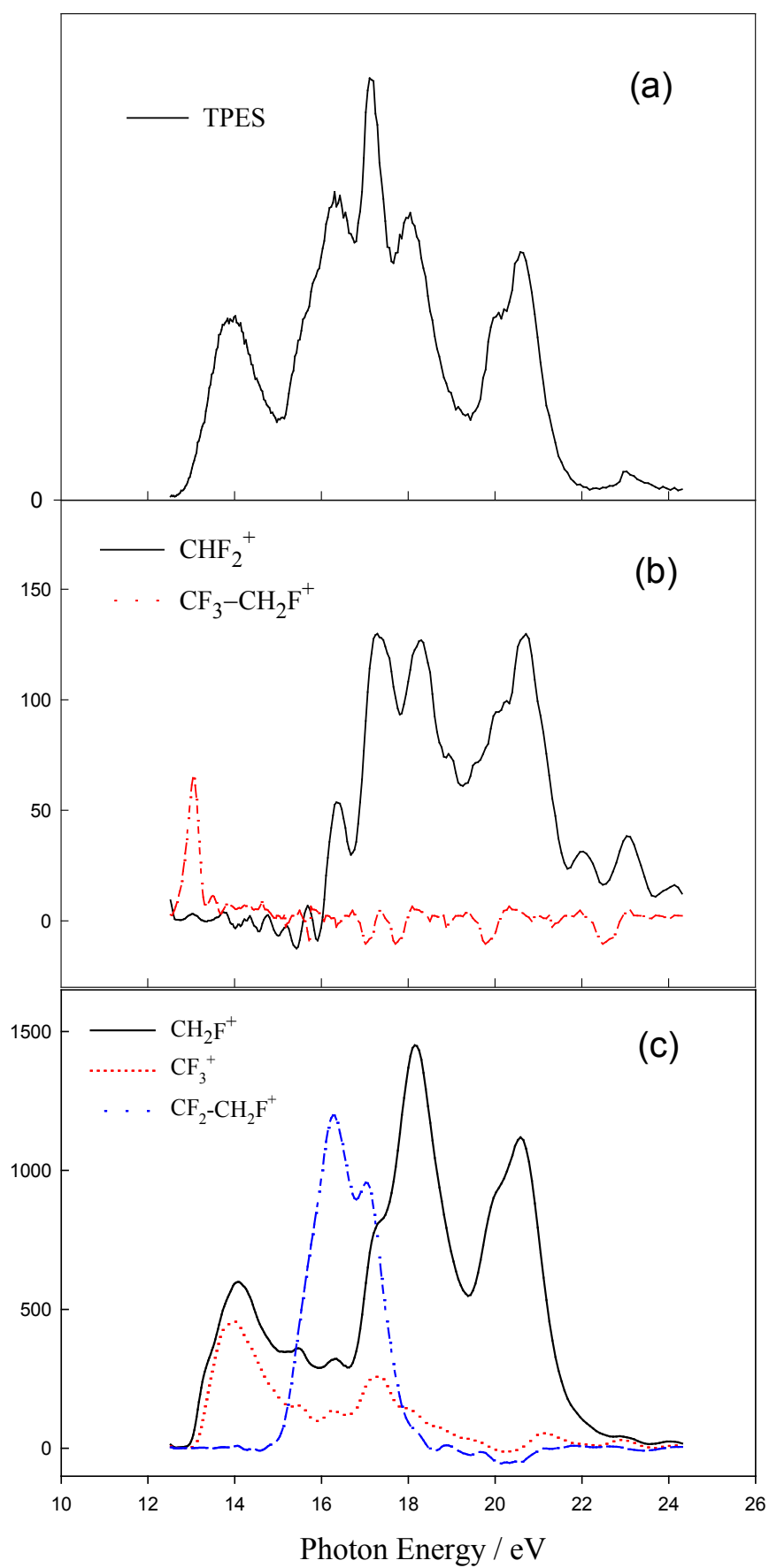**Figure 2**



Structure of neutral



7b$_u$ (*i.e.* HOMO-1)



8a$_g$ (*i.e.* HOMO)



7a$_g$ (*i.e.* HOMO-2)

**Figure 3**

**Figure 4**
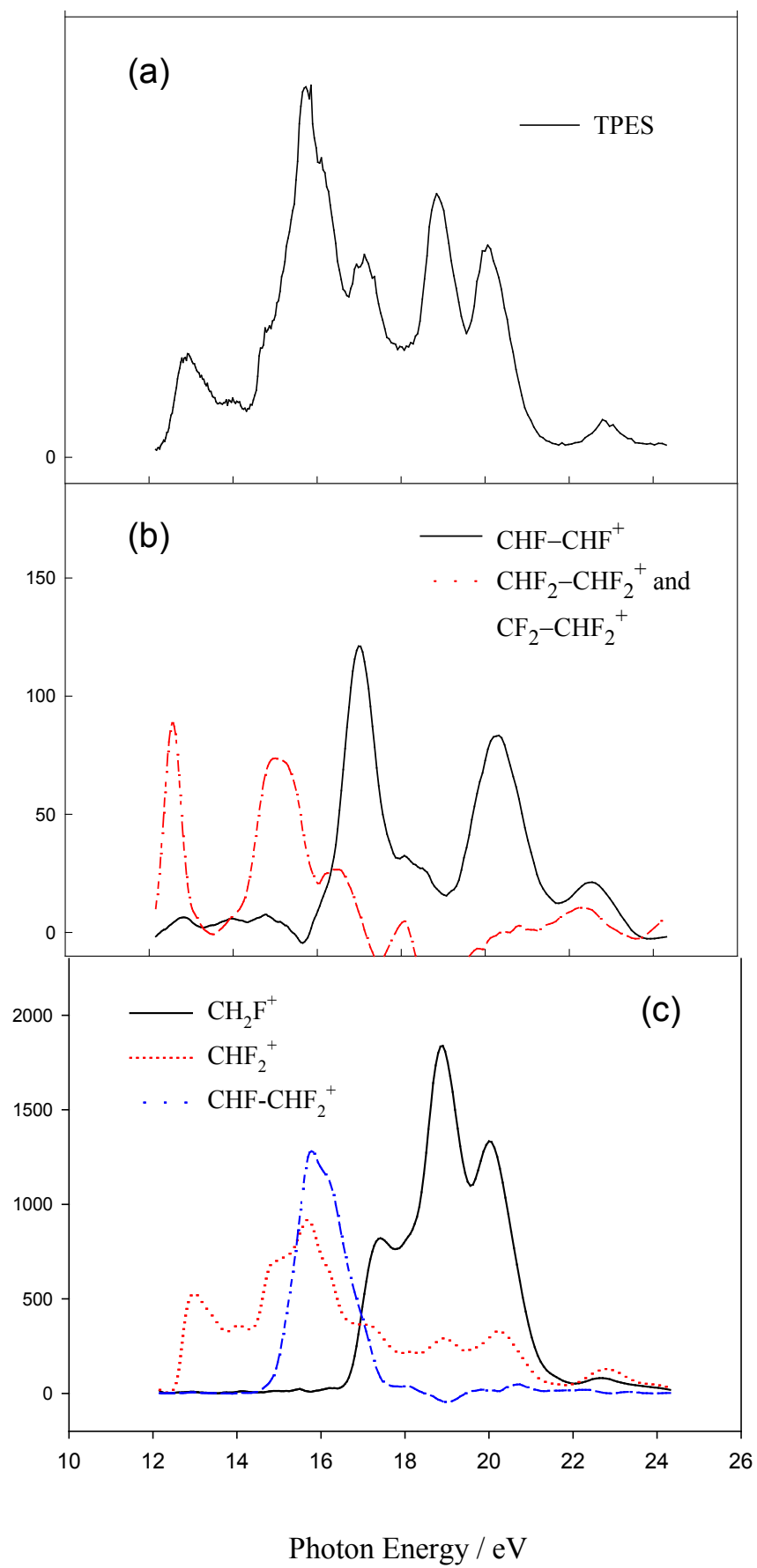
**Figure 5**

**Figure 6**

**Figure 7**



(a)      $\langle KE \rangle_T = 0.95 +/- 0.02$ eV

(b)